

Some remarkable properties of Hamiltonian matrices

A. P. Zuker, L. Waha Ndeuna, F. Nowacki, and E. Caurier,
IRES, Bât27, IN2P3-CNRS/Université Louis Pasteur BP 28, F-67037 Strasbourg Cedex 2, France
(May 19, 2019)

Continuous binomials are shown to reproduce the exact level densities—with the possible exception of the yrast state—at fixed angular momentum J for two families of realistic shell model diagonalizations. The elements of the Lanczos tridiagonal matrices that generate the spectra turn out to have general forms depending on the same parameters that determine the level density (first three moments and dimensionality of the space). Finally, the influence of the ground state position on thermodynamic quantities will be examined.

21.10.Ma,21.60.Cs,21.60.-n

Since many physical problems can be thought as matrix diagonalizations, much attention has been devoted to the general properties of matrices, starting with Wigner's Gaussian Orthogonal Ensemble (GOE) which has proven invaluable in providing insight into fluctuation properties [1]. To study level densities—and hence thermodynamic properties—it is necessary to enforce the condition that the Hamiltonians be of rank (r) 1+2 (i. e., 1+2-body). (In GOE the rank is the dimensionality of the space. Two Body Random Ensemble (TBRE) or Embedded GOE (EGOE) are the suggested denominations for limited ranks. We shall prefer to speak of Hamiltonian matrices.) Exact results become difficult to obtain, but early simulations strongly suggested that as the number of particles, n , exceeds r , the level densities rapidly evolve from the semicircular GOE form to a gaussian one when the Hamiltonian matrix elements are randomly chosen [2,3]. Even in the case of realistic Hamiltonians the gaussian seemed to do reasonably well [4,5]. The general proof that the spectrum is normally distributed [6] followed. It was recently suggested that this important result should be reinterpreted, by replacing gaussians by continuous binomials [7]. Our first aim is to test this proposal by comparing with exact diagonalizations (at fixed angular momentum J) for ^{48}Ca , a typical spherical nucleus [8], and for the configurations $(f_{7/2}p_{3/2})^4_{\pi}(g_{9/2}d_{5/2})^4_{\nu}$ ($(fpgd)^8$ for short) that exhibit rotational behaviour with backbend [9]. Once the test is passed, the structure of the tridiagonal matrices from which the spectra are calculated will be shown to have a remarkable form.

We borrow from [7] the binomial density (bin or b for short)

$$\begin{aligned} \lambda^k \binom{N}{k} &\Rightarrow \text{bin}(x, N, \lambda) \equiv \rho_b(x, N, \lambda) \\ &\approx \sqrt{\frac{8}{\pi N}} \exp [-(N-1)(x \ln x + \bar{x} \ln \bar{x}) + Nx \ln \lambda], \quad (1) \end{aligned}$$

where $x = k/N$, $\bar{x} = 1 - x$. For bin, the normalization, $(1 + \lambda)^N$, is missed by $\approx 2\%$ at small N , and should be corrected accordingly.

Setting $E = k\varepsilon - \Delta$, calling d the dimensionality of the basis, and d_0 the number of states at $x = 0$, the lowest moments are

$$d = d_0(1 + \lambda)^N, \quad E_c = \frac{N\varepsilon\lambda}{1 + \lambda} - \Delta, \quad (2)$$

$$m_2 = \sigma^2 = \frac{N\varepsilon^2\lambda}{(1 + \lambda)^2}, \quad \bar{m}_3 = \frac{m_3}{\sigma^3} = \gamma_1 = \frac{1 - \lambda}{\sqrt{N\lambda}}. \quad (3)$$

By combining the expressions for d and γ_1 , the equation

$$\frac{(1 - \lambda)^2}{\lambda} \ln(1 + \lambda) = \gamma_1^2 \ln(d/d_0). \quad (4)$$

determines λ , then N is extracted from d and ε from σ^2 . E_c is the position of the centroid with respect to the lowest (yrast) state of given J , taken to be at $E = 0$. The origin of the binomial is then at $-\Delta$. It is convenient to write $x = E/S$, where $S = N\varepsilon = \sigma(1 + \lambda)\sqrt{(N/\lambda)}$ is the spectrum span.

Figure 1 compares exact and binomial densities for a typical symmetric case ($\lambda = 1$), using the natural choice $d_0 = 1$.

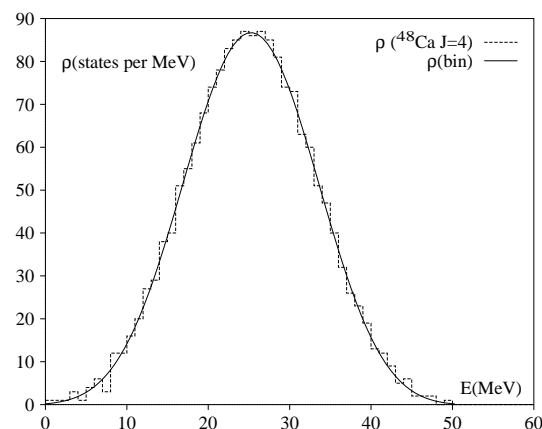


FIG. 1. Exact level densities ($d_0 = 1$, 1 MeV steps) for ^{48}Ca ($J = 4$) compared $\rho(\text{bin}) = \rho_b((E + \Delta)/S, N, \lambda)$ (parameters from Table I).

For asymmetric distributions ($\lambda \neq 1$) $d_0 = 1$ remains the sound choice, but the number of states at $x = 1$ can become very large: $d_N = d_0 \lambda^N$, leading to the abrupt stop of the binomial at high energy seen in Fig 2: The agreement is as good as in Fig. 1 up to well beyond the centroid, but the normalization to d becomes too large, since many exact states are missed. The correction can be made without introducing an *ad hoc* parameter.

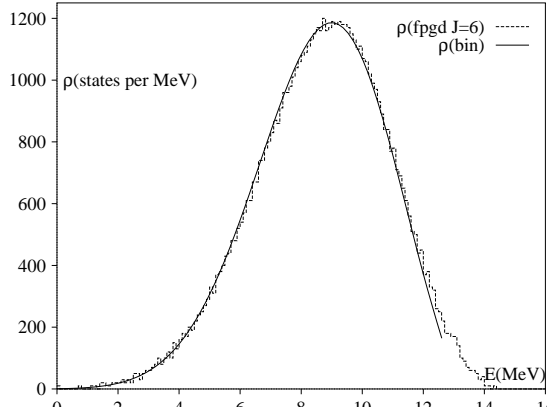


FIG. 2. Exact level densities compared with the $d_0 = 1$ variant for $(fpgd)^8$ ($J = 6$). 100 keV steps. Parameters from Table I for $\rho(\text{bin}) = \rho_b((E + \Delta)/S, N, \lambda)$.

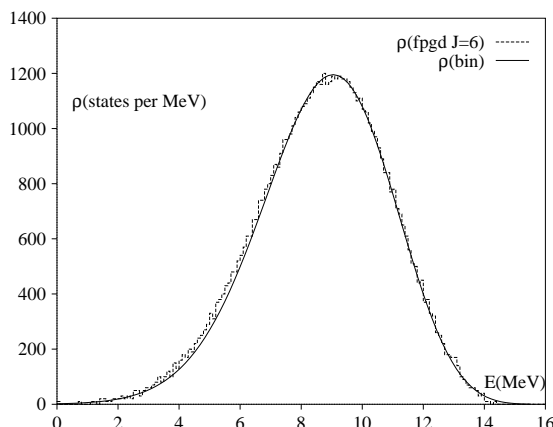


FIG. 3. As in Fig 2 but for the $d_N = 1$ variant.

To do so, first note that the normalization condition can be written as $d = d_0(1 + \lambda)^N = d_N(1 + 1/\lambda)^N$. Then choose $d_N = 1$. The result is shown in Fig 3. The parameters are strange, and in the first 57.25 MeV the binomial is negligible ($d_0 \approx 10^{-90}$), but it does a very good job, even at low energies. The normalization problem for the $d_0 = 1$ option, is solved by adjusting its maximum to that of the $d_N = 1$ case. (Done in Fig. 2)

It is worth noting that because of the factor $N - 1$ in the exponential of Eq. (1), the maximum of the density is shifted with respect to the centroid when $\lambda \neq 1$.

TABLE I. Lowest moments and parameters for the distributions in ^{48}Ca ($J = 4$) and $(fpgd)^8$ ($J = 6$) (in this case, the upper row corresponds to $d_0 = 1$, and the lower row to $d_N = 1$).

J	d	E_c	σ^2	γ_1	N	λ	S	Δ
4 ^{48}Ca	1755	25.24	61.66	-.01	10.55	1.04	51.02	.65
6 $(fpgd)^8$	6579	8.66	4.74	-.30	7.56	2.23	12.92	.22
6 $(fpgd)^8$	6579	8.66	4.74	-.30	92.24	10.11	72.77	57.25

The two spectra we have examined correspond to the maximal dimensionalities in each space. The agreement remains of the same quality as long as $d \gtrsim 300$. In ^{48}Ca it is still good for $J = 11$ ($d = 151$), and even $J = 12$ ($d = 73$).

Table II lists the binomial parameters for all the J values. When referred to the exact ground state—to calculate the total (scalar) density at the bottom of the table—the centroids in ^{48}Ca exhibit some odd-even staggering, and parabolic trends, but they are contained in the interval 29.9 ± 0.2 MeV. For $(fpgd)^8$, there is little staggering, and the expression $9.35 - 0.0085J(J + 1)$ is accurate to within 100 keV.

TABLE II. Binomial parameters ($d_0 = 1$) extracted from the lowest moments and dimensionality for all J values in ^{48}Ca and $(fpgd)^8$ (except $J = 22$, a single state)). The bottom line corresponds to the total scalar density ($d^{-1} \sum (2J + 1) \rho_J$).

J	^{48}Ca				$(fpgd)^8$			
	N	λ	S	Δ	N	λ	S	Δ
0	7.64	1.15	48.0	-4.00	5.43	2.53	11.97	-.66
1	11.34	.82	54.5	2.17	6.66	2.27	12.38	.82
2	10.69	1.00	53.2	.91	6.73	2.45	12.85	-.07
3	11.09	.96	52.7	.48	7.16	2.31	12.88	1.07
4	10.55	1.04	51.0	.65	7.22	2.36	13.03	.15
5	10.44	1.00	48.8	.26	7.51	2.22	12.94	.82
6	9.92	1.08	46.7	2.49	7.56	2.23	12.92	.22
7	9.75	1.04	44.0	1.97	7.83	2.05	12.75	.76
8	8.91	1.12	40.8	1.61	7.81	2.02	12.61	.22
9	8.64	1.05	37.6	2.42	8.07	1.86	12.36	.67
10	7.89	1.07	34.0	1.77	7.97	1.83	12.09	.19
11	7.14	1.00	28.8	2.06	8.18	1.67	11.75	.55
12	6.28	1.00	25.8	.80	7.96	1.65	11.36	.16
13	3.81	1.25	16.1	1.24	7.98	1.53	10.85	.49
14	3.14	.77	11.0	.20	7.41	1.58	10.18	.09
15					7.33	1.46	9.53	.46
16					6.34	1.59	8.59	.04
17					6.02	1.47	7.76	.53
18					4.87	1.68	6.57	-.07
19					4.39	1.48	5.44	.39
20					2.90	1.90	4.27	-.01
21					2.32	1.31	2.58	.14
$\sum[J]$	16.28	1.05	58.6	.15	13.53	1.75	16.4	1.86

The binomial level densities are excellent for all states, except for the lowest (yrast) ones, missed by the quantity Δ in table II. This anomaly is associated to a general feature of the tridiagonal matrices constructed in the Lanczos or Givens-Hauseholder algorithms used to generate the spectra [10]. The matrix elements depend on a starting vector, the pivot. *This dependence happens to be restricted to the lowest $M \times M$ submatrix, whose lowest eigenvalue is the exact one with good precision. $M \approx N/2$ when the pivot is the lowest state in the basis, when it is the highest, $M \lesssim 2N$. These numbers are so much smaller than d , that when the full matrix is represented, as in Fig. 4, only the general (pivot-independent) trend is visible.* The Lanczos algorithm provides a good formal framework to understand the behaviour of the matrix at the origin [7]. Here, we concentrate on the general trend.

To within fluctuations the diagonals in Fig. 4 are constant, and the off-diagonals have an inverse binomial form. The function $x = \text{nib}(y, N)$ is defined as the inverse of $y = (\pi N/2)^{-1/2} 2^{-N} \text{bin}(x + 1/2, N, 1)$, $x \geq 0$ (i. e., bin shifted and normalized so as to have maximum $y(0, N) = 1$). The precise statement is:

Given N and S (for $\lambda = 1$), $H_{ii+1} \approx (S/2)\text{nib}(i/d, N)$.

In Fig. 4 it is also seen that the corresponding inverse gaussian ($\sqrt{-2(\sigma/2)^2 \ln(i/d)}$) is quite close to nib, but the agreement will deteriorate for larger N .

The value $H_{01} = (S/2)\text{nib}(0, N) = S/4$ can be understood in terms of Gershgorin's theorem: Defining the segments (intervals) $G_i = (G_i^<, G_i^>)$, where $G_i^< = H_{ii} \mp (H_{ii+1} + H_{ii-1})$, the theorem states that the eigenvalues are contained in the segments (i. e., $\bigcup\{G_i\}$) [11, chapter 15]. Hence $\min\{G_i^<\}$ is a lower bound for the spectrum. In our case H_{ii} is constant, and the bound is at $H_{01} + H_{12} \equiv S/2$ below it, i. e., at the origin of the binomial. Therefore, upon diagonalizing the matrix with the nib form, the level density is undistinguishable from the corresponding bin, *except for the ground state* which comes a bit higher. Note that in Table II this is generally the case ($\Delta > 0$).

For the asymmetric case, $(fpgd)^8$ ($J = 6$), things are only slightly more complicated. First N and S are calculated for $\lambda = 1$, and the off-diagonals are initialized with these values, $H_{ii+1} \approx 7.75\text{nib}(i/6579, 12.68)$. The diagonals (referred to their centroid) are initialized by $H_{ii} \approx -\gamma_1(\ln(i/6579) + 1)$ ($-\gamma_1 = .295$). Then the values of S and γ_1 are corrected by solving

$$dm_2 = \langle \mathcal{H}^2 \rangle = \sum H_{ii+1}^2 + H_{ii-1}^2 + H_{ii}^2, \quad (5)$$

$$dm_3 = \langle \mathcal{H}^3 \rangle \simeq \sum H_{ii}(3H_{ii+1}^2 + 3H_{ii-1}^2 + H_{ii}^2). \quad (6)$$

The results, given in the caption of Fig. 5, do not differ much from the initializations. The inverse gaussian deviates more significantly from the binomial than in Fig. 4 (though hard to see because of the scale).

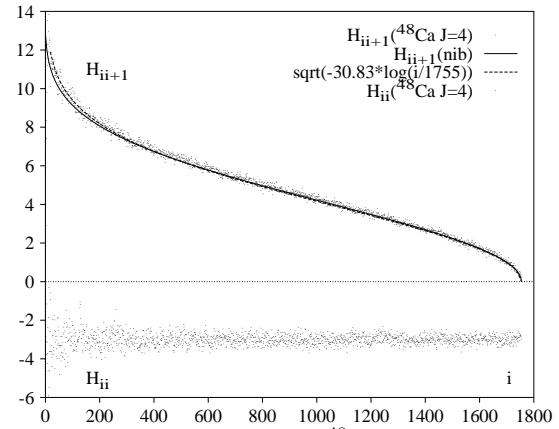


FIG. 4. Exact matrix elements for ^{48}Ca ($J = 4$) and the inverse binomial ($H_{ii+1} = 25.51\text{nib}(i/1755, 10.55)$) and inverse gaussian approximations for the off-diagonals.

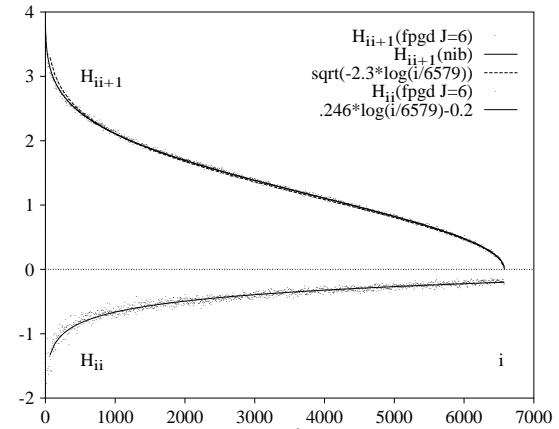


FIG. 5. Exact matrix elements (only one every ten are plotted) for $(fpgd)^8$ ($J = 6$) compared with $H_{ii} = .246 \ln(i/6579)$ (arbitrarily shifted), $H_{ii+1} = 7.64\text{nib}(i/6579, 12.68)$, and inverse gaussian.

It may be obvious—but it is worth stressing—that nothing has been *fitted*: the binomial densities and the tridiagonal matrix elements have been *calculated* in terms of the lowest moments and the dimensionality for each matrix. It could be expected that the results generalize. They could be characterized as CATs (Computer Assisted Theorems) waiting for a proof.

The nib and ln forms can be viewed as defining an integrable problem, leading to locally uniform level spacings and strength distributions that fluctuations will transform into Wigner spacings and localized strength [12]. The level densities are rigidly fixed, to within the uncertainty in the location of the yrast state. To assess the effect of this uncertainty we propose to examine the thermodynamic properties of ^{48}Ca , derived from the *total* density, very well described by the corresponding binomial from Table II, which—curiously—now locates the ground state at the correct position. (For $(fpgd)^8$ the

binomial is also excellent but now the ground state is badly missed.)

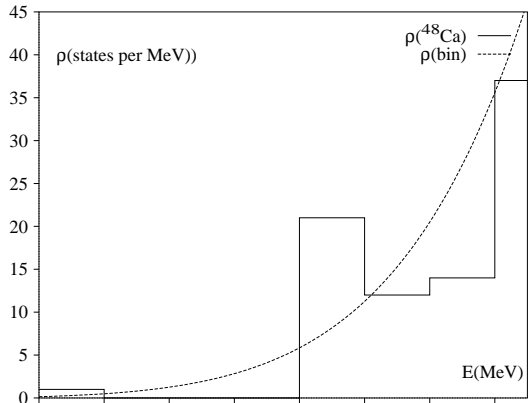


FIG. 6. Exact and binomial level density for the low lying states in ^{48}Ca .

Fig. 6 shows the situation near the origin.

The canonical thermodynamic functions are obtained from the partition function $Z = \rho(\beta) = \sum_E \rho(E) E^{-\beta E}$, and the averages $\langle E^\mu \rangle = Z^{-1} \sum_E E^\mu \rho(E) E^{-\beta E}$. Then the thermal energy and specific heat are ($\beta = 1/T$)

$$E = \langle E \rangle, \quad C = \frac{\partial E}{\partial T} = \beta^2 [\langle E^2 \rangle - \langle \langle E \rangle \rangle^2] \quad (7)$$

They are plotted in Fig. 7 for the exact results with the ground state displaced by different amounts δ (full lines) with respect to the correct value ($\delta = 0$, diamonds). The analytic values for a discrete binomial follow from Eqs. (2,3),

$$E_b = \frac{\varepsilon N}{2} \{1 - \tanh [\varepsilon/2T - \ln(\lambda)/2]\}, \quad (8)$$

$$C_b = N(\varepsilon/2T)^2 \operatorname{sech}^2 [\varepsilon/2T - \ln(\lambda)/2]. \quad (9)$$

The same results (within a $(1 - 1/N)$ factor) obtain from the microcanonical treatment ($\beta = \partial \ln \rho / \partial E$) of a continuous binomial. The near coincidence with the $\delta = 0$ curves is fortuitous, and due to the near coincidence between the energy step, ε , and the gap between ground state and excited states (≈ 4 MeV). The sensitivity of C and E to small variations δ is striking, in particular through the appearance of a second maximum below the Shottky peak [13] for $\delta < \varepsilon$. However, this peculiar behaviour is likely to be restricted to small spaces. For large N such anomalies should disappear.

For the cases considered here, gaussians are close enough to binomials to yield reasonable densities. For large N , when canonical and microcanonical quantities coincide, the situation will deteriorate. Since $\ln \rho_g(E) = -(E - E_c)^2/2\sigma^2$, we find $E_g = \max(E_c - \sigma^2/T, 0)$, and the specific heat is then $C_g = (\sigma/T)^2$ if $T > \epsilon/2$ and vanishes for $T < \epsilon/2$, a clearly unphysical discontinuity.

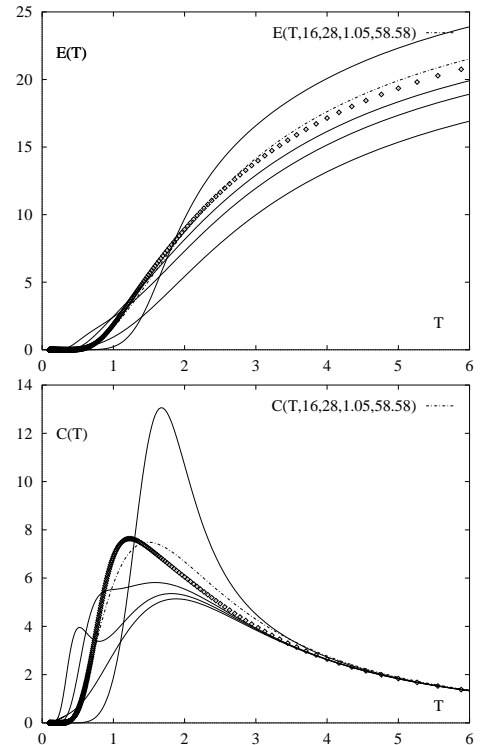


FIG. 7. Energies and specific heat for ^{48}Ca . diamonds: exact values; full lines (from top to bottom): exact values obtained by displacing the ground state by $\delta = -3, 1, 2, 4$ MeV; dot-dashes: Eqs. (8,9) with parameters from last row in table II.

- [1] *Statistical theories of spectra: Fluctuations*, C. E. Porter (Ed.), Academic Press, New York, 1965.
- [2] J. B. French and S. S. M. Wong, *Pys. Lett.* **33B**, 449 (1970), **35B**, 5 (1971).
- [3] O. Bohigas and J. Flores, *Pys. Lett.* **34B**, 261 (1971), **35B**, 383 (1971)
- [4] K. F. Ratcliff, *Phys. Rev.* **C3** (1971) 117.
- [5] M. Chang and A. P. Zuker, *Nuc. Phys.* **A198**, 417 (1972).
- [6] K. K. Mon and J. B. French, *Ann.Phys.(NY)* **95**, 90 (1975).
- [7] A. P. Zuker, previous letter.
- [8] E. Caurier, A.P. Zuker, A. Poves and Martinez-Pinedo, *Phys Rev C* **50**(1994)225.
- [9] A. P. Zuker, J. Retamosa, A. Poves and E. Caurier, *Phys. Rev. C* **52** (1995) R1741.
- [10] J. H. Wilkinson, *The algebraic eigenvalue problem*, OUP (1965).
- [11] I. S. Gradshteyn et I. M. Ryzhik *Table of Integrals, Series, and Products*. Academic Press (1979).
- [12] L. Waha Ndeuma, Ph.D thesis, IReS 99-16, Strasbourg (1999).
- [13] O. Civitarese, G. Dussel and A. P. Zuker, *Phys. Rev. C* **40** (1989) 2900.